Comparison of positive and negative compact intracloud discharges

Ting Wu,[1] Wansheng Dong,[1] Yijun Zhang,[1,2] and Tao Wang[1]

Received 22 October 2010; revised 19 November 2010; accepted 21 December 2010; published 15 February 2011.

[1] Prior studies have found that positive and negative compact intracloud discharges (+CIDs and −CIDs, according to the physics sign convection) occur at distinctly different altitudes, which correspond to different regions in a thunderstorm. On the basis of a large number of CIDs of both polarities recorded by our VLF/LF lightning location network, characteristic differences between +CIDs and −CIDs are discussed in this study. The results reveal that −CID is a more special type of discharge. Compared with +CIDs, −CIDs produce larger electric field changes on average, and they are more isolated from other discharge processes. A locating method based on ionospheric reflection pairs of CIDs is developed, which confirms that −CIDs do occur at higher altitudes. The relationship between CIDs and convective strength is also analyzed. Out of nine storms analyzed in this study, eight produce fewer −CIDs than +CIDs. The percentage of −CIDs seems to increase with the convective strength. Although −CIDs are relatively rare, their occurrences are more temporally compact; that is, a large portion of −CIDs are produced in a very short period. +CIDs also have this characteristic, but it is not as pronounced as that of −CIDs.

Citation: Wu, T., W. Dong, Y. Zhang, and T. Wang (2011), Comparison of positive and negative compact intracloud discharges, *J. Geophys. Res.*, *116*, D03111, doi:10.1029/2010JD015233.

1. Introduction

[2] CIDs are a distinct class of intracloud discharge processes. They are accompanied by powerful radiation in the HF and VHF radio bands [*Le Vine*, 1980; *Smith et al.*, 1999a; *Jacobson*, 2003], and they also produce large electric field changes that are comparable to that produced by return strokes [*Le Vine*, 1980; *Cooray and Lundquist*, 1985; *Willett et al.*, 1989; *Smith et al.*, 1999a]. CIDs are usually found isolated with other discharge processes at a time scale of several milliseconds [*Willett et al.*, 1989; *Smith et al.*, 1999a, 2002]. However, *Rison et al.* [1999] observed 13 CIDs which were all followed by other intracloud discharges within 10 ms. Further research indicated that at least a portion of CIDs are probably the initial events of lightning flashes [*Betz et al.*, 2008]. CIDs can be conveniently observed from the satellite [*Holden et al.*, 1995; *Light and Jacobson*, 2002] and thus may serve as a proxy of global convective activity for satellite-based remote sensing, so there has been a growing interest in the association between CIDs and severe tropospheric convection in recent years. It is generally agreed that CID rates are statistically correlated with convective strength, although there are still many uncertainties [*Suszcynsky and Heavner*, 2003; *Jacobson and Heavner*, 2005; *Wiens et al.*, 2008]. CIDs are also called "narrow bipolar events" or NBEs because of their narrow and bipolar radiation field pulses [e.g., *Willett et al.*, 1989].

[3] *Smith et al.* [2004] calculated heights of over 100,000 CIDs and they found that +CIDs occurred between 7 and 15 km and −CIDs occurred between 15 and 20 km. The result indicates that −CID is probably a type of discharge that occurs between upper positive charge region and the screening charge layer where normal intracloud discharges rarely occur. Therefore, it can be speculated that +CIDs and −CIDs are produced in largely different meteorological context and many of their characteristics may also be different from each other. Unfortunately, as far as we know, there are few studies concerning the differences between +CIDs and −CIDs. In this paper, we present observations of both polarities of CIDs by multiple stations of fast electric field change meters and discuss differences in multiple characteristics of +CIDs and −CIDs comprising the large peak electric field changes, temporal isolation, height of occurrence and their relationship with convective strength.

2. Data

[4] In the summer of 2007, a VLF/LF lightning location network consisting of 7 stations of fast electric field change meters were established in Guangzhou, China. All the electric field change meters were identical to each other and were similar in principle to that described by *Kitagawa and Brook* [1960]. The electric field change system had a decay time constant of 1 ms. The output was digitized at 10 MHz with a resolution of 12 bits and each record had duration of 1 ms. The software-based triggering system was similar to

[1]Laboratory of Lightning Physics and Protection Engineering, Chinese Academy of Meteorological Sciences, Beijing, China.
[2]State Key Laboratory of Severe Weather, Chinese Academy of Meteorological Sciences, Beijing, China.

0148-0227/11/2010JD015233

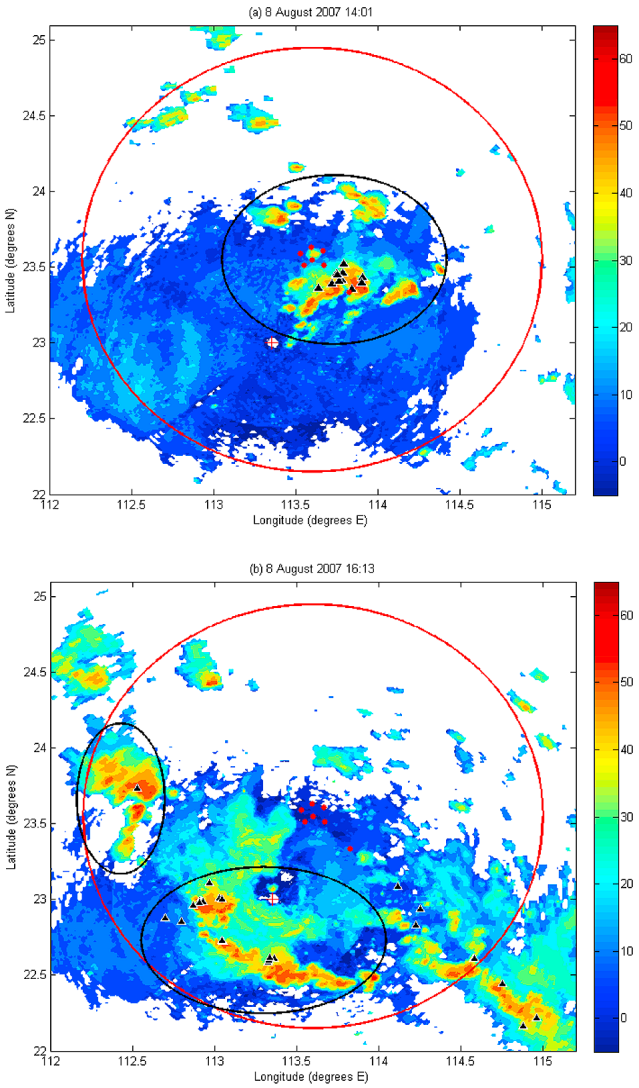

Figure 1. Composite radar reflectivity with locations of CIDs within 6 min of the radar time. Red dots represent observation stations. Red plus sign represents the radar station. Black triangles represent CIDs. The red circle represents an equidistance of about 150 km from the central station. Black circles are to illustrate the cell creation procedure discussed in section 3.4.

that of the upgraded LASA (Los Alamos Sferic Array) [*Shao et al.*, 2006], using floating trigger thresholds to prevent disturbance of fluctuating background noise. Continual data transmission from the digitizer to PC memory ensured that every electric field change signal exceeding the threshold value could be recorded without any dead time. Each recorded event was time stamped with GPS receivers, and three-dimensional position of the sources can be determined employing differential time-of-arrival (DTOA) technique.

[5] Five peripheral stations were located about 10 km to the central station, and a remote station was located about 32 km away from the central station. These seven stations are represented by red dots in Figure 1. Such a compact configuration is largely different from that of other lightning location systems such as LASA [*Shao et al.*, 2006], which has baselines of larger than 100 km. The compact configuration of our network can provide thorough and specified observations of those storms passing over. There is also an obvious limitation, though, that the location accuracy is relatively low for the discharges far away. Figure 1 shows two images of composite radar reflectivity with locations of CIDs within 6 min of the radar time. As in Figure 1a, the storm is close to the stations and all the CIDs are located at the high-reflectivity core. In Figure 1b, the storm is more than 100 km away from the stations, and some of the CIDs are located out of the high-reflectivity core. However, the result is still generally reasonable.

[6] Classification criteria for CIDs are similar to those employed by *Smith et al.* [2002] and *Hamlin et al.* [2007]. For each discharge event, if the mean pulse width of waveforms recorded by all the stations is ≤ 7 μs, and if the maximum of posttrigger SNR value is ≥ 23 dB, then the event is determined as a CID.

[7] In this paper, records of 19 days (from 6 August to 24 August) are used. There are 14 storm days in this period. A total of 11,876 CIDs was recorded comprising 7882 +CIDs and 3994 −CIDs. Physics sign convention for electric field change polarity is used throughout this paper, thus a negative cloud-to-ground return stroke produces a negative polarity field change signal. Typical waveforms of +CIDs, −CIDs and negative return strokes (−RSs) are shown in Figure 2. Differences between CIDs and −RSs are obvious, and ionospheric reflection pairs of CIDs are easily discerned. Note that the scale of electric field changes was not calibrated so the digital unit (DU) is used throughout this paper.

3. Results

3.1. Peak Amplitude of Electric Field Changes

[8] Peak amplitudes of electric field changes produced by +CIDs and −CIDs are compared with that of 138,148 −RSs observed during the same period similar to previous studies [*Le Vine*, 1980; *Willett et al.*, 1989; *Smith et al.*, 1999a]. In order to use the simple 1/R distance relation to normalize electric field change amplitude, only those discharge events located more than 50 km away from the central station are used to calculate the geometric mean value of electric field changes. The geometric mean values of electric field changes normalized to 100 km are 353, 506 and 187 DU for +CIDs, −CIDs and −RSs, respectively.

[9] In order to analyze the distribution of electric field changes, the value of 0–3000 DU is divided into 60 segments with 50 DU interval, and the value of larger than 3000 DU is set as another segment, thus totally 61 segments. Then the percentage of events that fall in each segment is calculated for +CIDs, −CIDs and −RSs. The result is shown in Figure 3. The distribution of −RSs is largely different from that of +CIDs and −CIDs, showing a predominant portion of −RSs having values below 500 DU. The normalized geometric mean value of −RSs is 187 DU, which is 0.53 of that of +CIDs and 0.37 of that of −CIDs. It seems that CIDs generally produce larger electric field changes than −RSs do. This result is in accordance with a recent study on +CIDs [*Nag et al.*, 2010].

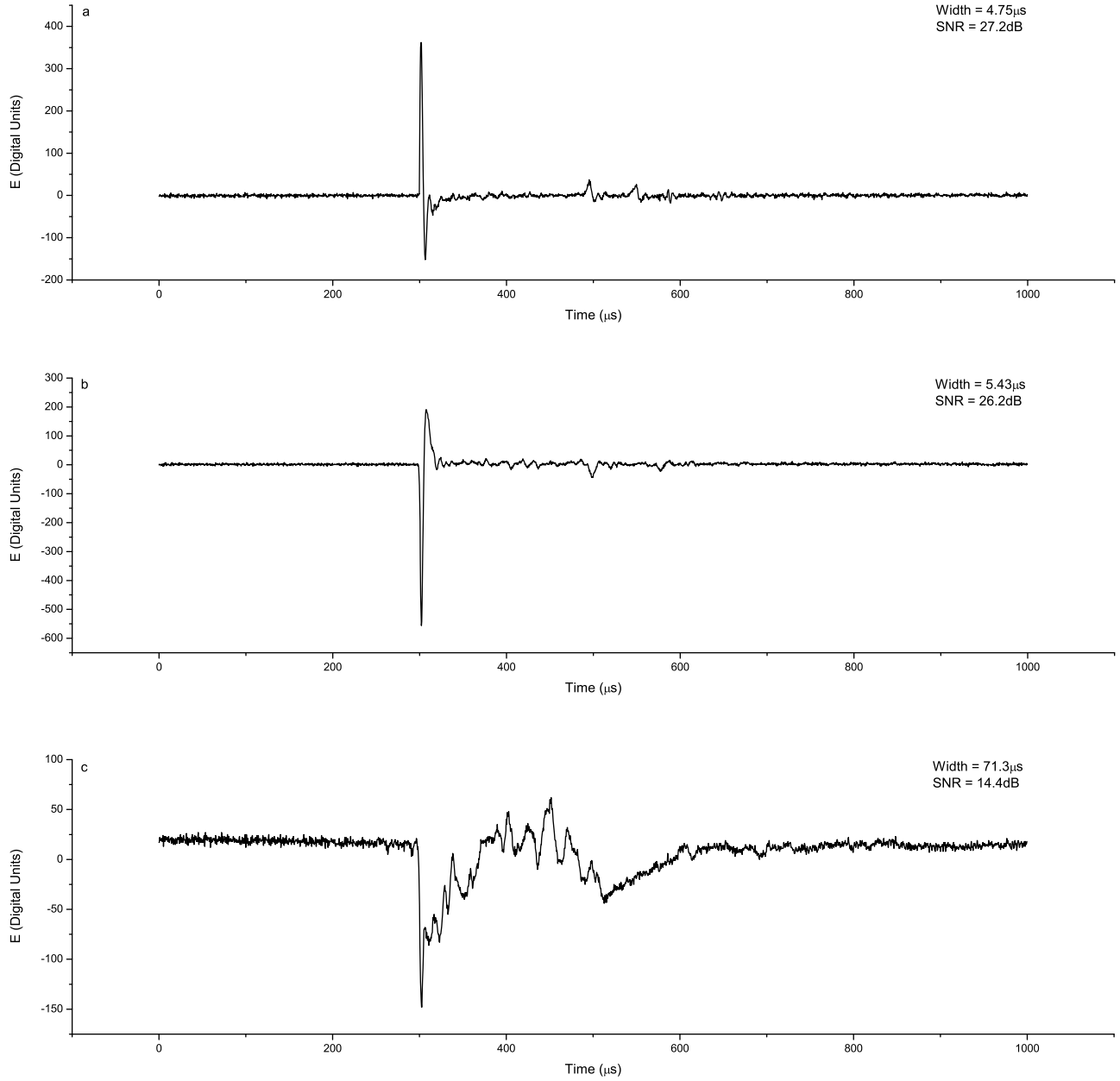

Figure 2. Typical waveforms of (a) +CIDs, (b) −CIDs, and (c) −RSs.

[10] Ratio of normalized mean value of +CIDs to −CIDs is 0.70. Their distributions of peak values have the same trend (Figure 3); the difference is in that a considerably higher percentage of −CIDs than +CIDs have large peak values of electric field changes. For example, there are 35% of −CIDs having peak values larger than 800 DU, compared with a value of 12% for +CIDs. Besides, there are 14 −CIDs with peak values larger than 3000 DU, while the maximum peak value of +CID is only 2900 DU. Therefore, −CIDs show a much higher possibility to produce very large electric field changes.

3.2. Temporal Isolation

[11] The characteristic of temporal isolation of CIDs has long been noticed [e.g., *Willett et al.*, 1989]. More recent observations indicate that at least a significant portion of CIDs serve as the initiation process of normal lightning [*Rison et al.*, 1999; *Betz et al.*, 2008]. However, it is still unclear to what extent are CIDs isolated with other discharge processes and whether there is any difference between +CIDs and −CIDs. In this study, on the basis of large samples of both +CIDs and −CIDs, we try to present some statistical results concerning the characteristic of temporal isolation of +CIDs and −CIDs.

[12] Since each waveform record in our study is 1 ms long, and other discharge pulses are rarely observed in the same record with a CID, we simply define the time difference between two discharge processes as the difference of trigger times of the two records. Considering the possibility that two or more independent discharge processes occur

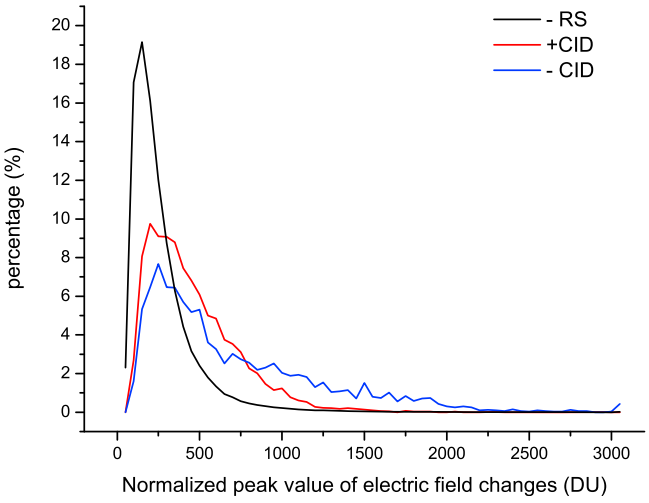

Figure 3. Distributions of normalized peak value of electric field changes of −RSs, +CIDs, and −CIDs. Each percentage is calculated by dividing the total number of events of each type by the number of events of this type that fall in each 50 DU long segment.

simultaneously at different places, we only consider records that are located within 20 km from each other to compute the time differences. Besides, the detection efficiency is relatively low for discharges far away and it is possible to detect CIDs while miss other discharges. In order to limit such detection bias, only those discharges located less than 100 km from the central station are considered. There are a total of 3205 +CIDs and 1969 −CIDs in this area.

[13] 11.7% of +CIDs are found to be followed by other discharge processes within 10 ms (defined as preceding-discharge percentage), and 1.6% of +CIDs occur within 10 ms after other discharge processes (defined as following-discharge percentage). The corresponding percentages for −CIDs are 4.4% and 1.7%. It is difficult to tell the distinguishable features merely from these values, but when comparing with the corresponding values of normal discharge processes, the significance of the results is obvious. There are a total of 244,989 triggering events in the analysis area, and normal discharge processes are picked out simply by excluding CID records from these triggering events. It is found that the preceding-discharge percentage of normal discharge processes is 13.0%, and the following-discharge percentage is 13.1%. Table 1 summarizes these results.

[14] The above results have twofold meaning. First, it is natural that the preceding- and following-discharge percentages of normal discharge processes are almost the same. However, by comparison, the preceding-discharge percentages of both polarities of CIDs are much larger than their following-discharge percentages. It indicates that both polarities of CIDs have much higher chance to serve as the initiation processes than to be initiated by other discharge processes. Second, the preceding-discharge percentage of +CIDs, which is close to that of normal discharge processes, indicates that a significant portion of +CIDs are indeed followed by other discharge processes. Such example is not difficult to find in our data set. Figure 4 shows an example of a +CID followed by typical intracloud discharges. The preceding-discharge percentage of −CIDs is much smaller than that of +CIDs, indicating that −CIDs are more likely to be temporally isolated from other discharge processes. This is in accordance with the observation by *Rison et al.* [1999] that all CIDs initiating normal intracloud discharges were positive polarity.

[15] It is interesting to note that of all the CIDs found to be associated with other discharge processes, 2 +CIDs precede −RSs, another 2 follow −RSs, 1 −CID precedes −RS, and 3 −CIDs follow −RSs. *Nag et al.* [2010] observed three +CIDs preceding CGs by 72–233 ms and 4 +CIDs during or after CGs based on 500 ms long electric field records, and distances between +CIDs and CGs were mostly less than 15 km. They also found 6 +CIDs occurring in pairs. It seems that CIDs can be associated with various kinds of discharge processes, although CIDs associated with normal intracloud discharges are significantly more common.

3.3. Ionospheric Reflection Pairs and Height of Occurrence

3.3.1. Method of 3-D Locating CIDs With Their Ionospheric Reflection Pairs

[16] The method of employing ionospheric reflection pairs to calculate source height of CIDs proposed by *Smith et al.* [1999a] is very useful for a lightning location system that is only capable of determining 2-D source locations like the one used in their work. It is also useful for a lightning location system that has very short baselines such as the one in our study. This method virtually adds some stations with very long baselines, so it can significantly increase the detection accuracy for discharges far away from the network.

[17] *Smith et al.* [1999a] employed ionospheric reflection pairs to calculate source height of CIDs and ionospheric virtual height after 2-D locations of CIDs had been determined. This method can be developed to calculate 3-D locations of CIDs and ionospheric virtual height simultaneously based on multiple-station observations. As in *Smith et al.* [1999a], we have the following relations according to Figure 5:

$$ct_{ia} = \sqrt{(2H - h - z_i)^2 + r_i^2} - \sqrt{(h - z_i)^2 + r_i^2} \quad (1)$$

$$ct_{ib} = \sqrt{(2H + h - z_i)^2 + r_i^2} - \sqrt{(h - z_i)^2 + r_i^2} \quad (2)$$

where t_{ia} is the arrival time difference of signal A and B, and t_{ib} is the arrival time difference of signal A and C. Both of t_{ia}

Table 1. Characteristics of Temporal Isolation

	Preceding-Discharge Percentage	Following-Discharge Percentage
+CID	11.7%	1.6%
−CID	4.4%	1.7%
Normal discharge process	13.0%	13.1%

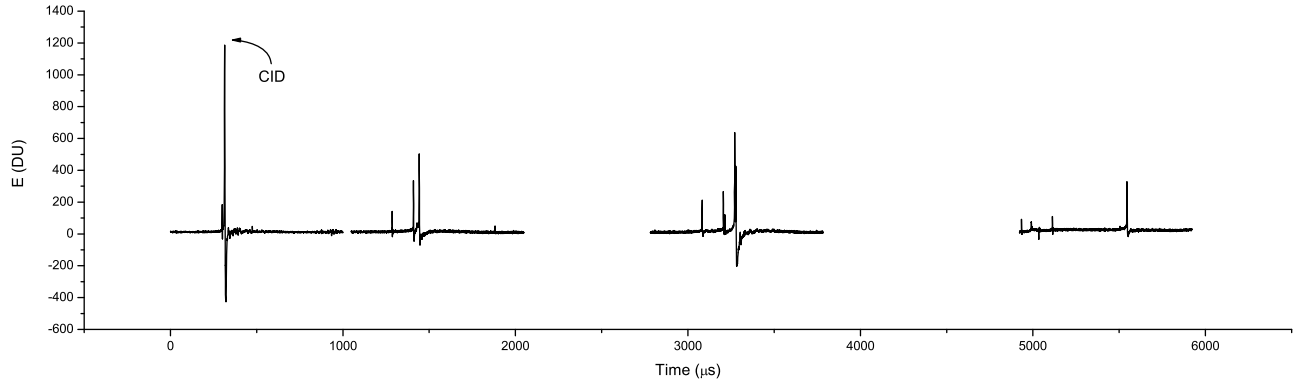

Figure 4. A CID followed by typical intracloud discharges. The distance between two successive discharge events calculated from their locations provided by the lightning location network is no larger than 3.5 km, which indicates that these discharges probably belong to the same process.

and t_{ib} can be measured directly from the waveforms. r_i is given by

$$r_i = R \cdot \arccos[\sin(x_0)\sin(x_i) + \cos(x_0)\cos(x_i)\cos(y_0 - y_i)] \quad (3)$$

where R is the radius of the Earth, x_0 and y_0 are the latitude and longitude of the source location, and x_i and y_i are the latitude and longitude of the ith station.

[18] In equations (1) and (2) the Earth is treated as a flat plane. In this study, CIDs with ionospheric reflection pairs are mostly observed between 100 km and 300 km from the network. The ones nearer cannot produce clear reflection pairs and the ones farther cannot be effectively detected. In this range, the error caused by the flat Earth model is around 100 m, which is trivial and can be neglected. Equation (3) is based on spherical coordinates rather than Cartesian coordinates because it turns out that such consideration does not significantly increase the complexity of calculation and it makes the result closer to reality.

[19] Substituting equation (3) into equations (1) and (2), the two equations have four unknowns, so records of two stations can provide a set of solutions. Since a discharge event is usually observed by 5 or more stations simultaneously, the optimization method is used to minimize the following function:

$$f(H, h, x_0, y_0) = \sum_{i=1}^{n}\left[ct_{ia} - \sqrt{(2H - h - z_i)^2 + r_i^2} + \sqrt{(h - z_i)^2 + r_i^2}\right]^2 + \left[ct_{ib} - \sqrt{(2H + h - z_i)^2 + r_i^2} + \sqrt{(h - z_i)^2 + r_i^2}\right]^2 \quad (4)$$

where n is the number of stations observing the same discharge event. A MATLAB function *fminsearch*, which uses the simplex search method [*Lagarias et al.*, 1998] to find the minimum of a multivariable function, is employed to minimize the function (4). In this way, 3-D location of CIDs and virtual ionospheric height are obtained.

3.3.2. Height of Occurrence of +CIDs and −CIDs

[20] In order to validate this method, results of locations of CIDs are compared with composite radar reflectivity. Figure 6 shows an image of composite radar reflectivity with CIDs that are located using their ionospheric reflection pairs. The storms are nearly 200 km away from the network. Although some of CIDs are located out of the

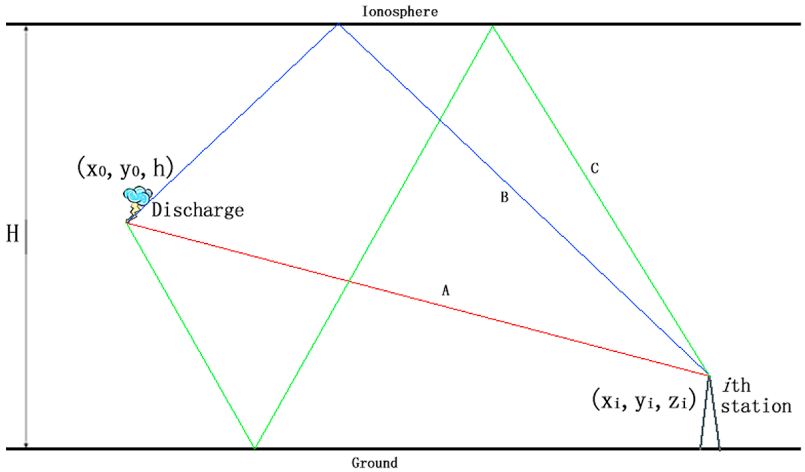

Figure 5. Illustration of the propagation paths of ionospheric reflection pairs of CIDs. A flat Earth model is used.

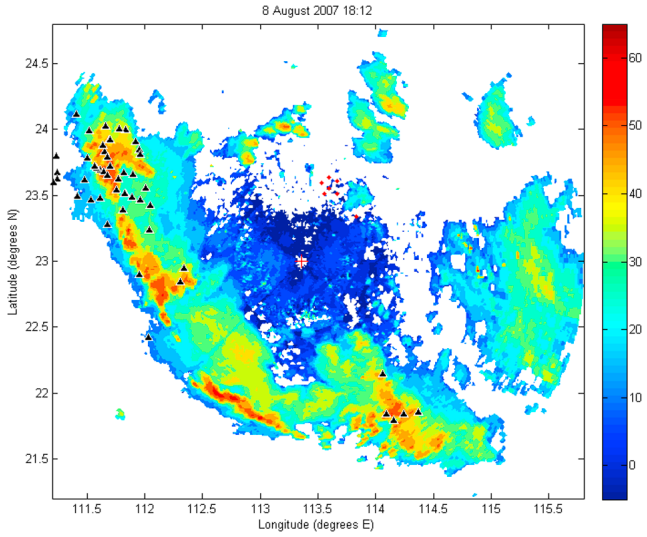

Figure 6. Composite radar reflectivity with locations of CIDs within 6 min of the radar time. Black triangles represent CIDs, which are located by their ionospheric reflection pairs. Red dots represent observation stations. Red plus sign represents the radar station.

high-reflectivity core, the result is generally satisfactory considering the long distances between the storms and the network and the small area that the network covers.

[21] Only results of source height (h) and ionospheric virtual height (H) for those CIDs that are located within the high-reflectivity cores are used because these results are most probably accurate. For example, CIDs located in white and blue areas in Figure 6 are not selected for statistics. In this way, a total of 555 +CIDs and 174 −CIDs are picked out manually by comparing with composite radar reflectivity. Their source heights and corresponding ionospheric virtual heights are scatterplotted in Figure 7. +CIDs and −CIDs show surprisingly distinctive source heights. Heights of most +CIDs range from 8 to 16 km with a geometric mean of 12 km, and heights of most −CIDs range from 16 to 19 km with a geometric mean of 17 km. This result agrees well with that of *Smith et al.* [2004], further demonstrating that +CIDs and −CIDs occur in distinctly different altitudes. It is worth noting that the highest CID in this study is 20.1 km, larger than the tropopause height of 16–17 km in the summer according to local sounding data. Several previous studies have also observed many CIDs occurring above 20 km and even as high as 30 km [*Smith et al.*, 2004; *Jacobson and Heavner*, 2005; *Nag et al.*, 2010]. Ionospheric virtual heights in this study are mostly between 85 km and 95 km. Since CIDs with ionospheric reflection pairs were all observed at night in this study, from about 1800 to 0600 local time, this result generally agrees with *Smith et al.* [2004] as well.

3.4. Percentage of −CIDs and Relationship With Convective Strength

3.4.1. Cell Creation Procedure

[22] In this study, the observation area is quite limited compared with previous studies [e.g., *Wiens et al.*, 2008] based on the data of LASA. In order to relate the CIDs with the storm producing them, only those storms and CIDs that are within 150 km from the central station are considered because within this range the location error is relatively small (see Figure 1). In this area, 9 storm processes are conveniently picked out according to the radar data. It is worth noting that since the analysis area is relatively small, the processes considered are not always going through the entire storm life; that is, a storm may not be formed within the area or may move out of the area in its later stage. In order to statistically study the relationship between CIDs and convective strength, the duration of each storm is divided into time windows of 6 min, equivalent to a complete volume scan of radar. However, the area is not divided into equivalent grids like in previous studies; instead, it is considered as a single zone unless it comprises multiple independent storms and each storm produces CIDs. Such treatment can ensure that each zone covers a separate storm. Each zone is treated as a data cell, and the number of both +CIDs and −CIDs and the maximum reflectivity of this data cell are calculated. For example, in Figure 1a, only one data cell is considered, while in Figure 1b, two data cells are considered (illustrated by black circles in Figure 1). In this way, a total of 698 data cells are obtained.

[23] Unlike previous studies, such a procedure creates data cells that do not have identical areas, but the areas usually do not differ a lot, and when the ratio of +CIDs to −CIDs is considered, difference of areas is not a problem. An obvious advantage of this procedure is that each data cell contains a separate storm and a single storm would not be divided into multiple data cells.

3.4.2. Percentage of −CIDs

[24] In all of 698 data cells, 416 contain at least one CID. Figure 8 shows the distribution of percentages of −CIDs (ratio of −CIDs to both polarities of CIDs) in each of these data cells. A pronouncing feature in Figure 8 is that there are 218 data cells containing only +CIDs, accounting for 52% of all data cells with at least one CID. Besides, 29 data cells

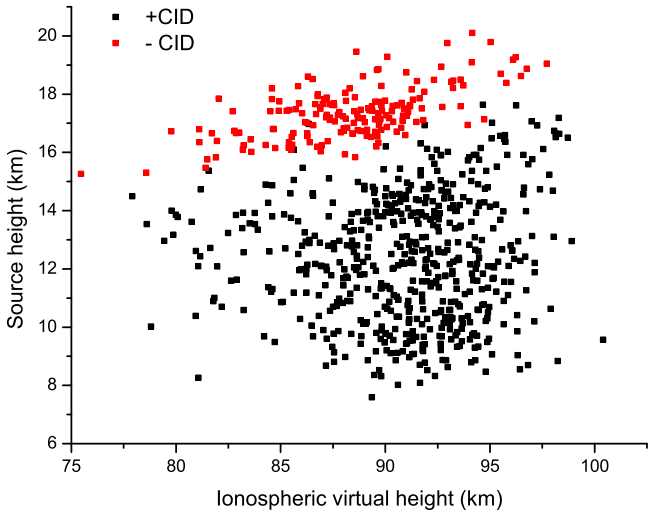

Figure 7. A scatterplot of source height of CIDs versus ionospheric virtual height. The results are computed by ionospheric reflection pairs. Only those CIDs located within high-reflectivity cores are included.

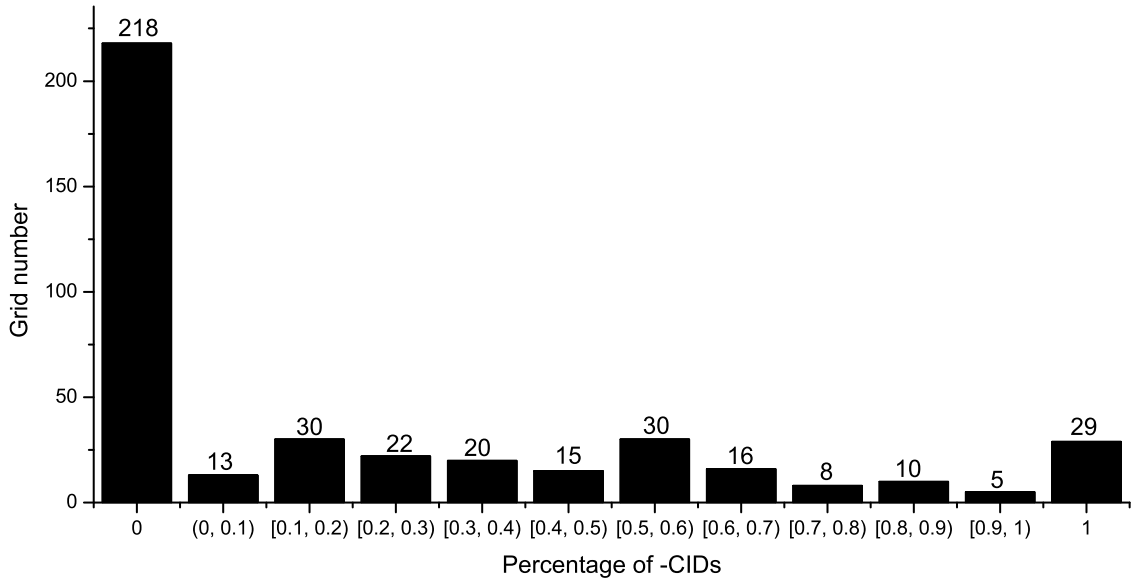

Figure 8. Distribution of percentages of −CIDs in each data cell.

contain only −CIDs. The number of data cells with only one polarity CIDs is 247, accounting for 59% of all data cells with at least one CID. From another perspective, the percentages of −CIDs in 9 storms in this study are 41%, 54%, 13%, 18%, 15%, 41%, 27%, 35%, 10%. Clearly most storms have more +CIDs than −CIDs, and both polarities of CIDs occur in the same storm. These results indicate that on a small time scale (6 min in this study), CIDs tend to occur as the same polarity; that is, CIDs of the same polarity tend to cluster in a short period. However, on the time scale of a storm, CIDs of both polarities are produced.

[25] Although +CIDs are more prevalent, the biggest number of −CIDs in one data cell is larger than that of +CIDs. The three largest numbers of −CIDs in one data cell are 95, 71, and 51. And the three largest numbers of +CIDs in one data cell are 67, 48, and 46. Three data cells have total duration of only 18 min, but they account for 19% and 7% of all −CIDs and +CIDs, respectively. This clearly demonstrates the temporal compactness of CID occurrences, which has also been pointed out by previous studies [e.g., *Jacobson and Heavner*, 2005]. And this result indicates that −CIDs are more pronounced than +CIDs in such characteristic.

3.4.3. Relationship With Convective Strength

[26] The number of CIDs and the maximum reflectivity of each data cell are scatterplotted in Figure 9. The red line connects the average number of CIDs with the same value of maximum reflectivity. The maximum reflectivity is obviously correlated with convective strength to some degree and has been employed by *Wiens et al.* [2008] to infer the relationship between CIDs and convective strength as well. Note that radar-derived storm top is not utilized here because the value appears inaccurate when the storm is very close to the radar station. Figure 9 shows that the average CID rate increases with the maximum reflectivity of below 58 dBZ. The large variation of CID rates when the maximum reflectivity exceeds 58 dBZ is probably because of small samples of data cells. This result is in accordance with previous studies [e.g., *Wiens et al.*, 2008] and also justifies the cell creation procedure in this study.

[27] Percentage of −CIDs in each storm varies considerably, from 10% to 54%. It seems that the percentage of −CIDs in a storm is connected with the convective strength. Figure 10 depicts the mean maximum reflectivity versus the percentage of −CIDs in each storm, and they are linearly fitted with a correlation coefficient of 0.62. The mean maximum reflectivity is calculated by averaging the maximum reflectivity of all data cells in a given storm. The trend for the mean maximum reflectivity to increase with the percentage of −CIDs is obvious. This result probably has certain associations with the fact that the heights of −CIDs are mostly larger than that of +CIDs. Since maximum reflectivity is related with convective strength and height of cloud top to some degree, this result may indicate that the higher a thunderstorm develops the greater possibility it has to produce −CIDs.

4. Discussion

[28] *Le Vine* [1980], when he observed CIDs for the first time, noticed that they were "relatively isolated." *Willett et al.* [1989] had the similar result, concluding that CIDs were not associated with any identified lightning process. *Smith et al.* [1999a] studied waveforms of CIDs produced by three thunderstorms and stated that CIDs were temporally isolated from other discharges on a time scale of several seconds to several tens of seconds within the same thunderstorm; that is, CIDs occurred as single discharges. There are also many studies concluding that CIDs are accompanied by other discharge processes. *Rison et al.* [1999], utilizing LMA (Lightning Mapping Array), observed 13 +CIDs and found that each +CID initiated an intracloud discharge within 10 ms. They stated that previous studies observed CIDs unaccompanied with any other discharge process because those measurements were primarily at large distances and they tended to miss small-amplitude processes of intracloud discharges. *Smith et al.* [1999b] also presents an

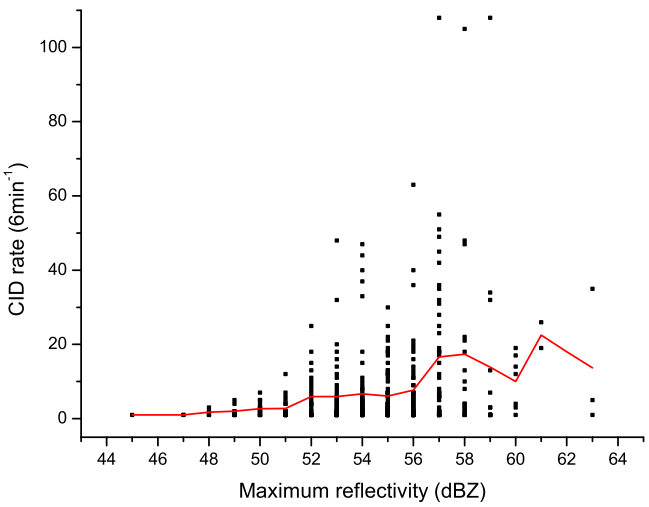

Figure 9. A scatterplot of CID rate versus maximum reflectivity for each data cell. The red line connects the mean value of CID rate of each value of maximum reflectivity.

example of a +CID followed by intracloud discharges. *Betz et al.* [2008] analyzed the first in-cloud events by both VLF/LF and VHF networks. They found that up to half of those events were almost simultaneously detected by both VLF/LF and VHF networks. The time differences between VLF/LF and VHF signals were often smaller than 100 μs. With large amplitudes of VLF/LF signals that were comparable to that of RSs, these time-coincident events were very likely CIDs. If this is true, then at least a significant portion of CIDs do initiate normal lightning. Results in our study also support that a portion of CIDs are indeed followed by other discharge processes. CIDs analyzed by *Smith et al.* [1999a] were mostly hundreds of kilometers away from the observation stations and it is very likely that some small-amplitude discharge processes following CIDs were not detected. It is interesting to note that instances of CIDs that are followed by other discharge processes presented by previous studies are all positive polarity, and the result of this study also shows that +CIDs are more likely to be followed by other discharge processes than −CIDs. Perhaps it is just a coincidence, but it is possible that discrepancy between +CIDs and −CIDs is larger than their preceding-discharge percentages indicate. It is even possible that when CIDs are found to be followed by other discharge processes, they are mostly +CIDs, while −CIDs rarely have such behavior. At last, a conclusion should be made, as indicated by the following-discharge percentages, that both +CIDs and −CIDs are much more likely to be initiation processes than to be initiated by other discharge processes.

[29] *Jacobson and Heavner* [2005] and *Wiens et al.* [2008] have both statistically studied the ratio of +CIDs to −CIDs in a given storm. *Jacobson and Heavner* [2005], on the basis of LASA observation in Florida, found that a given storm rarely produced both polarities of CIDs. However, *Wiens et al.* [2008] found that both polarities of CIDs often occurred in the same storm in Great Plains. *Hamlin et al.* [2009] stated that the difference of CID production in Great Plains versus Florida possibly indicated the difference in the storms themselves. However, it should be noted that both analyses by *Jacobson and Heavner* [2005] and *Wiens et al.* [2008] were based on grid cells having duration of 10 min. We have already demonstrated that at a short time scale CIDs tend to be of single polarity. In this study, 59% of 6 min data cells have only one polarity of CIDs, which is likely corresponding to the result of *Jacobson and Heavner* [2005]. It seems that both of the above analyses could only show the ratio of +CIDs to −CIDs at a time scale of 10 min instead of a given storm. For 9 storms in this study, every storm produces both polarities of CIDs, and it is very likely that for a given storm in both Florida and Great Plain, it also produces both polarities of CIDs. Further research on some specific storms in these areas are needed to solve this issue.

5. Conclusions

[30] This study focuses on differences between +CIDs and −CIDs which have rarely been investigated by previous studies. It has been discovered that, compared with +CID, −CID is a more special type of discharge in the following respects.

[31] 1. −CIDs produce, on average, larger electric field changes than +CIDs do.

[32] 2. Larger portion of −CIDs than that of +CIDs are temporally isolated with other discharge processes on a time scale of 10 ms.

[33] 3. −CIDs mostly occur at higher altitudes than +CIDs do. Most of −CIDs occur between 16 and 19 km, while most of +CIDs occur between 8 and 16 km.

[34] 4. −CIDs are generally rarer than +CIDs. Eight out of 9 storms in our analysis produce more +CIDs than −CIDs. But both +CIDs and −CIDs occur in every storm.

[35] 5. Considering some short periods that have largest rates of +CIDs or −CIDs, there are significantly larger portion of −CIDs than that of +CIDs occurring in these periods. It indicates that −CIDs' occurrences are more temporally compact.

[36] 6. The percentage of −CIDs in a given storm has the trend to increase with the convective strength.

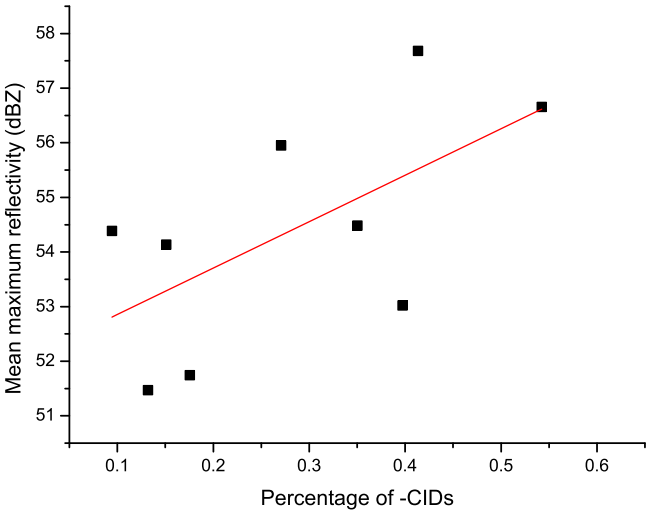

Figure 10. A scatterplot of the mean maximum reflectivity versus percentage of −CIDs in each storm. The mean maximum reflectivity is calculated by averaging the maximum reflectivity of all data cells in a given storm.

[37] These differences are related with each other. Supported by the result of *Smith et al.* [2004], it is almost certain that −CIDs occur at higher altitudes (the third difference). Some −CIDs even occur above the nominal tropopause [*Jacobson and Heavner*, 2005]. This requires the thunderstorm producing them to be extremely vigorous and the cloud top to be very high, which is likely related with the sixth difference. Besides, the region where −CIDs occur probably corresponds to the region between upper positive charge layer and the screening charge layer, where normal lightning discharges can rarely occur, while the region where +CIDs occur is almost the same as the region where normal intracloud discharges are usually observed. This may determine that −CIDs are more temporally isolated with other discharge processes (the second difference).

[38] Since −CIDs are often accompanied by extremely vigorous storms, such vigorous storms usually provide large power, which may be responsible for −CIDs' larger electric field changes (the first difference) and extremely high rates in some short periods (the fifth difference). At the same time, such vigorous state can hardly last for a long time, which makes −CIDs relatively rarer (the fourth difference).

[39] The above explanation is of course more of a conjecture. Since the mechanism of CIDs is not quite clear yet, it is impossible to explain these characteristics explicitly. The differences we have found, however, surely distinguish −CIDs from +CIDs in many aspects. More work is needed to reveal the physical mechanisms responsible for these differences between +CIDs and −CIDs.

[40] **Acknowledgments.** This work was supported in part by the National Natural Science Foundation of China under grants 41075022 and 40875003 and the Ministry of Science and Technology under grant 2008EG137292. The authors thank Xuan-Min Shao for constructive comments on this paper. Valuable suggestions from three anonymous reviewers are also acknowledged.

References

Betz, H.-D., T. C. Marshall, M. Stolzenburg, K. Schmidt, W. P. Oettinger, E. Defer, J. Konarski, P. Laroche, and F. Dombai (2008), Detection of in-cloud lightning with VLF/LF and VHF networks for studies of the initial discharge phase, *Geophys. Res. Lett.*, *35*, L23802, doi:10.1029/2008GL035820.

Cooray, V., and S. Lundquist (1985), Characteristics of the radiation fields from lightning in Sri Lanka in the tropics, *J. Geophys. Res.*, *90*(D4), 6099–6109, doi:10.1029/JD090iD04p06099.

Hamlin, T., T. E. Light, X. M. Shao, K. B. Eack, and J. D. Harlin (2007), Estimating lightning channel characteristics of positive narrow bipolar events using intrachannel current reflection signatures, *J. Geophys. Res.*, *112*, D14108, doi:10.1029/2007JD008471.

Hamlin, T., K. C. Wiens, A. R. Jacobson, T. E. Light, and K. B. Eack (2009), Space- and ground-based studies of lightning signatures, in *Lightning: Principles, Instruments and Applications*, edited by H. Betz, U. Schumann, and P. Laroche, pp. 287–307, Springer, Berlin.

Holden, D. N., C. P. Munson, and J. C. Devenport (1995), Satellite observations of transionospheric pulse pairs, *Geophys. Res. Lett.*, *22*(8), 889–892, doi:10.1029/95GL00432.

Jacobson, A. R. (2003), How do the strongest radio pulses from thunderstorms relate to lightning flashes?, *J. Geophys. Res.*, *108*(D24), 4778, doi:10.1029/2003JD003936.

Jacobson, A. R., and M. J. Heavner (2005), Comparison of narrow bipolar events with ordinary lightning as proxies for severe convection, *Mon. Weather Rev.*, *133*, 1144–1154, doi:10.1175/MWR2915.1.

Kitagawa, N., and M. Brook (1960), A comparison of intracloud and cloud-to-ground lightning discharges, *J. Geophys. Res.*, *65*(4), 1189–1201, doi:10.1029/JZ065i004p01189.

Lagarias, J. C., J. A. Reeds, M. H. Wright, and P. E. Wright (1998), Convergence properties of the Nelder-Mead simplex method in low dimensions, *SIAM J. Optim.*, *9*(1), 112–147, doi:10.1137/S1052623496303470.

Le Vine, D. M. (1980), Sources of the strongest RF radiation from lightning, *J. Geophys. Res.*, *85*(C7), 4091–4095, doi:10.1029/JC085iC07p04091.

Light, T. E. L., and A. R. Jacobson (2002), Characteristics of impulsive VHF lightning signals observed by the FORTE satellite, *J. Geophys. Res.*, *107*(D24), 4756, doi:10.1029/2001JD001585.

Nag, A., V. A. Rakov, D. Tsalikis, and J. A. Cramer (2010), On phenomenology of compact intracloud lightning discharges, *J. Geophys. Res.*, *115*, D14115, doi:10.1029/2009JD012957.

Rison, W., R. J. Thomas, P. R. Krehbiel, T. Hamlin, and J. Harlin (1999), A GPS-based three-dimensional lightning mapping system: Initial observations in central New Mexico, *Geophys. Res. Lett.*, *26*(23), 3573–3576, doi:10.1029/1999GL010856.

Shao, X. M., M. Stanley, A. Regan, J. Harlin, M. Pongratz, and M. Stock (2006), Total lightning observations with the new and improved Los Alamos sferic array (LASA), *J. Atmos. Oceanic Technol.*, *23*, 1273–1288, doi:10.1175/JTECH1908.1.

Smith, D., X. M. Shao, D. N. Holden, C. T. Rhodes, M. Brook, P. R. Krehbiel, M. Stanley, W. Rison, and R. Thomas (1999a), A distinct class of isolated intracloud lightning discharges and their associated radio emissions, *J. Geophys. Res.*, *104*(D4), 4189–4212, doi:10.1029/1998JD200045.

Smith, D. A., R. S. Massey, K. C. Wiens, K. B. Eack, X. M. Shao, D. N. Holden, and P. E. Argo (1999b), Observations and inferred physical characteristics of compact intracloud discharges, in *Proceedings of the 11th International Conference on Atmospheric Electricity*, edited by H. Christian, *NASA Conf. Publ.*, *209261*, 6–9.

Smith, D. A., K. B. Eack, J. Harlin, M. J. Heavner, A. R. Jacobson, R. S. Massey, X. M. Shao, and K. C. Wiens (2002), The Los Alamos sferic array: A research tool for lightning investigations, *J. Geophys. Res.*, *107*(D13), 4183, doi:10.1029/2001JD000502.

Smith, D. A., M. J. Heavner, A. R. Jacobson, X. M. Shao, R. S. Massey, R. J. Sheldon, and K. C. Wiens (2004), A method for determining intracloud lightning and ionospheric heights from VLF/LF electric field records, *Radio Sci.*, *39*, RS1010, doi:10.1029/2002RS002790.

Suszcynsky, D. M., and M. J. Heavner (2003), Narrow bipolar events as indicators of convective strength, *Geophys. Res. Lett.*, *30*(17), 1879, doi:10.1029/2003GL017834.

Wiens, K. C., T. Hamlin, J. Harlin, and D. M. Suszcynsky (2008), Relationships among narrow bipolar events, "total" lightning, and radar-inferred convective strength in Great Plains thunderstorms, *J. Geophys. Res.*, *113*, D05201, doi:10.1029/2007JD009400.

Willett, J. C., J. C. Bailey, and E. P. Krider (1989), A class of unusual lightning electric field waveforms with very strong high-frequency radiation, *J. Geophys. Res.*, *94*(D13), 16,255–16,267, doi:10.1029/JD094iD13p16255.

W. Dong, T. Wang, T. Wu, and Y. Zhang, Laboratory of Lightning Physics and Protection Engineering, Chinese Academy of Meteorological Sciences, Beijing 100081, China. (wuting@cams.cma.gov.cn)